

The role of fluid pressure on frictional behavior at the base of the seismogenic zone

Greg Hirth^{1*} and N.M. Beeler²

¹Department of Earth, Environmental and Planetary Sciences, Brown University, Providence, Rhode Island 02912, USA

²U.S. Geological Survey, Vancouver, Washington 98683, USA

ABSTRACT

To characterize stress and deformation style at the base of the seismogenic zone, we investigate how the mechanical properties of fluid-rock systems respond to variations in temperature and strain rate. The role of fluids on the processes responsible for the brittle-ductile transition in quartz-rich rocks has not been explored at experimental conditions where the kinetic competition between microcracking and viscous flow is similar to that expected in the Earth. Our initial analysis of this competition suggests that the effective stress law for sliding friction should not work as efficiently near the brittle-ductile transition as it does at shallow conditions.

INTRODUCTION

Applications of the effective stress law indicate that pore fluid pressure controls fault strength (e.g., Hubbert and Rubey, 1959) as well as physical properties relied on to constrain the mechanical state of fault zones, such as acoustic velocity, poroelasticity, and electrical conductivity. High fluid pressures are also invoked to explain the low frequency range of slip behaviors observed for seismogenic faults, such as episodic tremor and slip observed near the base of the seismogenic zone along both the San Andreas fault near Parkfield (California, USA) and the Cascadia thrust interface (e.g., Thomas et al., 2012). Despite our appreciation of the potential role of fluids in these environments, an experimental foundation for effective stress at these higher-temperature conditions is lacking. Here we describe a new approach for characterizing the evolution of effective stress with depth at conditions near the base of the seismogenic zone.

Our motivation comes from three observations that collectively suggest that the standard definition of effective normal stress for fault slip, $\sigma_{\text{eff}} = (\sigma_n - P_f)$, where σ_n is normal stress and P_f is fluid pressure, may not hold near the base of the seismogenic zone. First, extrapolation of quartzite flow laws indicates that the brittle-ductile transition (BDT) occurs at $\sim 300^\circ\text{C}$ at geologic strain rates for conditions where fault strength is controlled by a coefficient of friction (μ) of 0.6 with a hydrostatic pore-fluid pressure gradient (where the ratio of pore-fluid pressure to lithostatic pressure [λ] is ~ 0.4) (Fig. 1). While a simplification of the broad range of processes that occur near the BDT, this canonical view (e.g., Brace and Kohlstedt, 1980; Sibson, 1983) is actually reinforced by improvements in flow laws and the analytical techniques used to investigate fault rocks. For example, Behr and Platt (2011) demonstrated that stress–temperature–strain rate conditions at the BDT on the long-lived Whipple Mountain detachment (Southern California) are consistent with a strength profile similar to that shown in Figure 1. Key elements of the microstructures preserved in such natural rocks (recrystallized grain size, dislocation density) indicate peak differential stresses during viscous flow in the range of 100–200 MPa near the BDT (e.g., Hirth et al., 2001; Stipp et al., 2002; Behr and Platt, 2011). Similarly, while depth resolution is poor, analyses of larger-scale dynamics indicate that stresses of ~ 100 MPa are possible (or even likely, depending on perspective) near the BDT along the San Andreas fault (e.g., Humphreys and Coblenz, 2007). These studies indicate that ductile flow, rather than friction, limit mid-crustal strength, requiring either low pore pressure (Fig. 1) or an ineffective pore-pressure relation.

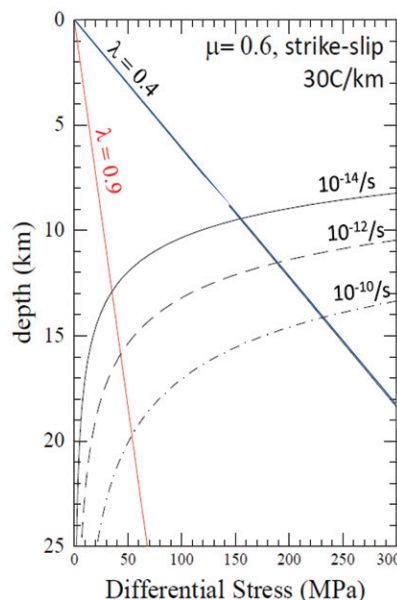


Figure 1. Differential stress versus depth for strike-slip setting showing brittle-ductile transition for different strain rates and pore-fluid pressures. Stresses in ductile regime (black curves) calculated using quartzite flow law (Hirth et al., 2001). Stresses in frictional regime calculated using coefficient of friction of $\mu = 0.6$ and ratios of pore pressure to lithostatic pressure of $\lambda = 0.4$ (hydrostatic pore-fluid pressure gradient, blue line) and 0.9 (near-lithostatic pore-fluid pressure gradient, red line). Such models predict relatively low stresses and dominantly brittle deformation for crustal conditions with high pore fluid pressure. Calculations are made assuming a geothermal gradient of $30^\circ\text{C}/\text{km}$.

Second, we suggest that the preservation of relatively high-stress microstructures indicates that the effective stress law must sometimes evolve rapidly near the BDT—again, becoming more ineffective with increasing depth. There is abundant evidence for the presence of fluids during viscous deformation of mylonites (e.g., recrystallization and redistribution of micas, dissolution and reprecipitation of quartz). Furthermore, analyses of fluid inclusions preserved in mylonites indicate near-lithostatic pore fluid pressures (e.g., Axen et al., 2001). Based on Figure 1, maintenance of high pore fluid pressure (leading to λ approaching 1) is incompatible with viscous creep stresses of 100–200 MPa. A similar “paradox” is evident at experimental conditions where viscous creep is studied in the laboratory. In this case, the presence of fluid (which should produce low effective stress) does not promote localized brittle failure (e.g., Chernak et al., 2009), even though these experiments are conducted under undrained conditions.

Third, experiments on partially molten rocks illustrate viscous creep behavior during both drained compaction and undrained triaxial deformation tests (e.g., Hirth and Kohlstedt, 1995; Renner et al., 2003), even though the melt pressure approaches or equals the confining pressure (from which one would predict stresses much lower than observed by applying the conventional effective stress law). In both cases, aggregate behavior is well fit by models that account for the grain-to-grain contact (or asperity) rheology—which is in turn modulated by the topology (or contiguity) of the fluid phase (e.g., Hirth and Kohlstedt, 1995; Takei and Holtzman, 2009).

ARE CHANGES IN α THE KEY TO UNDERSTANDING THE BDT?

The effect of pore-fluid pressure on mechanical behavior in the frictional regime is described using the relationship:

$$\sigma_{\text{eff}} = (\sigma_n - \alpha P_f), \quad (1)$$

where for most applications the constant α is assumed to be unity. However, at high pressure-temperature conditions, where creep and crack

*E-mail: greg_hirth@brown.edu

healing processes are efficient, α may decrease significantly. Owing to the exponential temperature dependence of thermally activated processes, changes in α may occur with relatively small spatial and/or temporal variations. In contrast, for rock failure and frictional sliding at low temperature and pressure, $\alpha \approx 1$ is nearly always observed (e.g., Handin et al., 1963; Morrow et al., 1992). During frictional sliding at low temperature, the real area of surface contact normalized by the nominal area of contact (A_r/A) is very small. Scholz (1990) noted that the effective stress controlling the strength of faults is related to the fractional area along a fault surface that is supported by pressurized pore space relative to the area that is supported by asperity contact across the fault. Where the area of contact is vanishingly small, a change in pore pressure within the fault acts in nearly exact opposition to the applied fault normal stress, implying:

$$\alpha = 1 - A_r/A \approx 1. \quad (2)$$

Dieterich and Kilgore (1996) hypothesized that A_r/A can be related to the rheological properties of the mineral grains using the relationship:

$$A_r/A = \sigma_n/\sigma_y, \quad (3)$$

where σ_n is the applied normal stress and σ_y is the yield stress at the frictional contacts, which is controlled by the indentation hardness at low temperature. However, at higher temperatures, σ_y decreases due to easier viscous creep, leading to an increase in A_r/A (e.g., Boettcher et al., 2007) and potentially a concomitant decrease in α .

To include temperature-dependent creep in the effective stress law for friction, we make two modifications to Equation 3. First, because Dieterich and Kilgore (1996) conducted their experiments dry, for fluid present conditions σ_n should be replaced by σ_{eff} giving:

$$\alpha \approx 1 - \sigma_{\text{eff}}/\sigma_y. \quad (4)$$

Second, A_r/A cannot exceed unity, thus Equation 4 is only applicable where $\sigma_y > \sigma_{\text{eff}}$.

The solution of Equations 1 and 4 is

$$\sigma_{\text{eff}} = \frac{(\sigma_n - P_f)}{1 - (P_f/\sigma_y)}, \quad (5)$$

which provides a first-order effective stress law for high-temperature rock friction.

APPLICATION

To illustrate the potential influence of α on stress in the Earth, we construct profiles of differential stress ($\Delta\sigma$) versus depth using the temperature- and strain-rate-dependent effective stress law, a constant $\mu = 0.6$, and a constant fluid pressure gradient defined by $\lambda = 0.4$. For a strike-slip environment, the differential stress in the frictional regime can be approximated by

$$\sigma_1 - \sigma_3 = \sigma = F'(\sigma_v - \alpha P_f), \quad (6)$$

where σ_v is the vertical stress resulting from overburden, and $F' = 2\mu/(\mu^2 + 1)^{1/2}$ (e.g., Zoback and Townend, 2001).

The $\Delta\sigma$ predicted by these relationships is shown in Figure 2A assuming $\sigma_n = \sigma_v$. We used a composite flow law for the asperity yield stress, $\sigma_y = [1/\sigma_{\text{glide}} + 1/\sigma_{\text{disl}}]^{-1}$, which accounts for dislocation glide (σ_{glide}) at low temperature (we used a constant yield stress of 2 GPa in the glide regime, guided by indentation hardness tests on quartz; Evans, 1984) and dislocation creep (σ_{disl}) at higher temperatures (we used the quartzite flow law of Hirth et al. [2001]). The resulting yield stress and α (Equation 4) are labeled in Figure 2A. At low temperature and pressure, where σ_y is large, and thus A_r/A is small, the predicted friction law follows the strength-depth relationship defined by a hydrostatic pore-fluid pressure

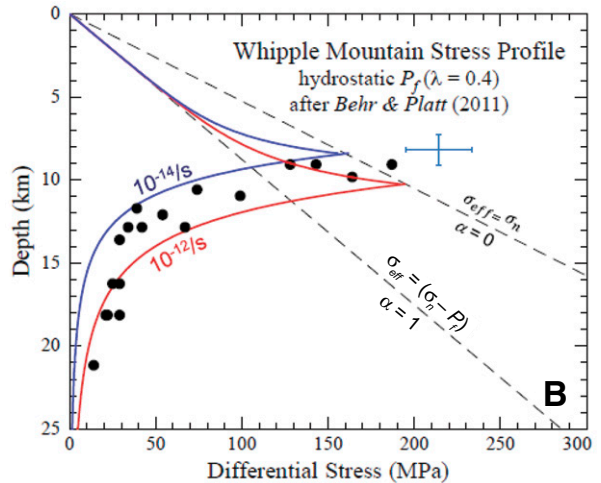
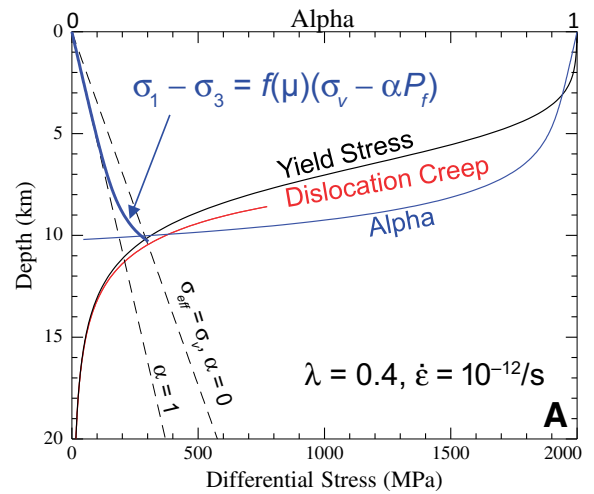


Figure 2. A: Transition in frictional behavior arising from decrease in alpha (α , the effective stress coefficient) with increasing temperature; frictional stress (from Equation 6) and magnitude of α (upper x-axis) are shown by blue curves. Yield stress at frictional asperities is shown by black curve. Yield stress and dislocation creep stress (red curve) were calculated for strain rate of $10^{-12}/\text{s}$ and ratio of pore pressure to lithostatic pressure of $\lambda = 0.4$. **B:** Comparison of stress based on temperature-dependent effective stress law with estimates based on grain size piezometry of quartz mylonites (representative errors shown by blue bars) from Whipple Mountain detachment (Southern California) (after Behr and Platt, 2011; see the GSA Data Repository¹). Plot is calculated for normal faulting setting (see the Data Repository) with strain rates of $10^{-12}/\text{s}$ and $10^{-14}/\text{s}$. Dashed lines in both A and B show frictional stress for an effective normal stress (σ_{eff}) with hydrostatic pore-fluid pressure (P_f) ($\lambda = 0.4$ and $\alpha = 1$) and with lithostatic normal stress ($\alpha = 0$).

gradient. However, α decreases with increasing temperature (owing to the temperature effect on creep—included in σ_y), and the friction law evolves toward that defined by a lithostatic pressure gradient near the BDT.

The value of α also depends on strain rate through the strain-rate dependence of σ_y . We assume a strain rate of $10^{-12}/\text{s}$ throughout the model in Figure 2. This choice is based on an active deformation width of ~ 1 km for a plate displacement rate of ~ 30 mm/yr ($\sim 10^{-9}$ m/s), consistent with the width of major crustal shear zones (e.g., Bürgmann and Dresen, 2008) and the width of microseismicity along faults in California (e.g., Powers and Jordan, 2010).

¹GSA Data Repository item 2015083, notes on differential stress calculations, is available online at www.geosociety.org/pubs/ft2015.htm, or on request from editing@geosociety.org or Documents Secretary, GSA, P.O. Box 9140, Boulder, CO 80301, USA.

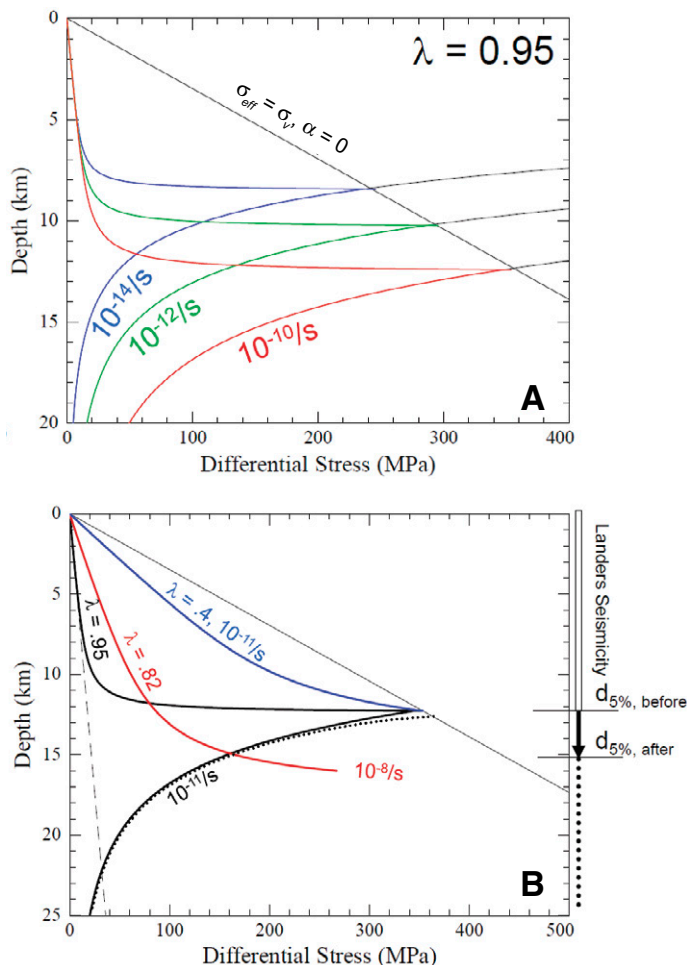


Figure 3. A: Differential stress versus depth with near-lithostatic pore-fluid pressure (ratio of pore pressure to lithostatic pressure of $\lambda = 0.95$), calculated for strike-slip setting. With higher strain rate, depth to brittle-ductile transition (BDT) increases and stress within brittle regime decreases, due to strain-rate dependence of α (Equation 4). Line labeled $\sigma_{\text{eff}} = \sigma_v$, $\alpha = 0$ shows frictional stress for α (effective stress coefficient) = 0. **B:** Trade-offs between pore-fluid pressure and strain rate. For constant strain rate, depth to BDT does not depend on pore-fluid pressure. Background strain rate of $10^{-11}/\text{s}$ is illustrated, for which BDT occurs at depth constrained by background seismicity rate at Landers, California, defined by average depth of deepest 5% of earthquakes, $d_{5\%,\text{before}}$ (Rolandone et al., 2004). Increase in depth to BDT after the 1992 Landers earthquake ($d_{5\%,\text{after}}$) can arise from increase in strain rate. Model with temperature-dependent α (red curve) shows that this transition can occur without increase in stress (at depth of ~15 km), even with modest decrease in pore-fluid pressure. In contrast, with $\alpha = 1$, stress increase much larger than predicted by co-seismic stress change (dotted black curve; based on Montési, 2004) is required to promote significant increase in depth to BDT (see Fig. 1). Dashed line shows frictional stress for $\lambda = 0.95$ and $\alpha = 1$. Gray line is the same as in A; black dots on lower right y-axis show the depth extent of microseismicity after the Landers earthquake.

As illustrated in Figure 2B, the resulting differential stress-depth diagram is consistent with geological constraints for stress in the earth. The stress just below the BDT (e.g., Behr and Platt, 2011) is well predicted by the dislocation creep flow law we employed to constrain σ_y . Values of differential stress greater than that predicted for a friction law with hydrostatic pore-fluid pressure have previously been interpreted to result from co-seismic stress increases (e.g., Behr and Platt, 2011). In contrast, the temperature-induced decrease in α suggests that such stresses may occur under nominally steady-state creep. For reference, relatively high stresses near the BDT have also been determined directly from borehole data and

microstructural observations of rocks from the KTB drill hole (Germany) (e.g., Dresen et al., 1997).

The onset of ductility, which promotes the increase in A_f/A , also leads to conditions where pore-fluid pressure increases (as fluids become isolated during compaction). To illustrate the potential implications of high fluid pressure, we show strength-depth profiles assuming a near-lithostatic pore-fluid pressure ($\lambda = 0.95$) in Figure 3A. Under these conditions, the temperature and strain-rate dependence of α result in an abrupt change from frictional to viscous behavior—and associated increase in differential stress. This scenario is consistent with evidence for high fluid pressure in mylonites mentioned above and allows for very weak faults in the brittle regime, but is a stark contrast to predictions based on the effective stress law for friction when the influence of temperature on α is not considered (i.e., Fig. 1). Figure 3A also shows that small changes in strain rate dramatically change the depth where brittle deformation is expected.

Accounting for variations in α also predicts surprising changes in the velocity (strain rate) dependence of friction (flow stress). Figure 3A illustrates that an increase in strain rate (causing an increase in yield stress) can result in a concomitant increase in α (see Equation 4), which results in a decrease in differential stress required for frictional sliding (because the effective stress law becomes “more effective”). Such behavior expands Scholz’s (1990) idea of the schizosphere (cf. Handy et al., 2007). Many mylonitic rocks show microstructural evidence for temporal changes between brittle and ductile behavior. The example in Figure 4 shows microcracks—defined by arrays of fluid inclusions—overprinting subgrain boundaries within viscously deformed quartz grains; the microcracks are in turn overprinted by dynamically recrystallized grains. These crosscutting relations suggest a sequence of viscous to brittle back to viscous deformation.

Changes in the depth of microseismicity following earthquakes suggest that increases in strain rate promote significant changes in the depth of the BDT. After the 1992 Landers earthquake (Southern California), microseismicity was observed at depths greater than 20 km, and the average depth of the deepest 5% of events ($d_{5\%}$) increased from ~12 to 15 km (Rolandone et al., 2004). Assuming standard stress-depth relationships, such as shown in Figure 1, the high strain rates required to promote the observed increase in depth of brittle deformation following the Landers earthquake would result in a significant increase in differential stress. However, this stress increase is much larger than predicted by calculations of the co-seismic stress change from the earthquake in the lower crust (compare Fig. 1 to Fig. 3B).

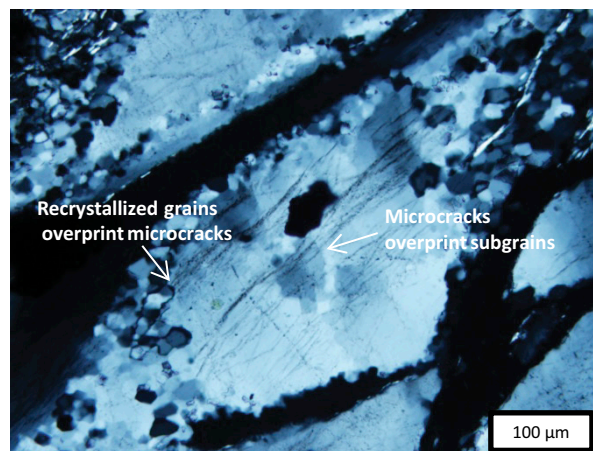


Figure 4. Optical micrograph of quartzite mylonite from Ruby Gap duplex (central Australia) (Hirth et al., 2001) with microstructure indicative of alternating brittle and viscous deformation; microcracks, defined by arrays of fluid inclusions, overprint subgrain boundaries within quartz porphyroclast; microcracks are in turn overprinted by dynamically recrystallized grains along grain boundaries.

An alternative explanation for the depth extent of earthquake-induced microseismicity may be that P_f remains near-lithostatic and that an increase in strain rate promotes microcrack growth, redistribution of fluid, and a transient increase in α . In this case, the increase in α could conceivably offset the local decrease in pore-fluid pressure associated with dilatant microcracking, leading to concomitant “strain rate weakening” (or “dilatancy weakening”)—and a transition to brittle deformation, a scenario which could lead to a dispersed zone of deep microseismicity. In Figure 3B, we show that the increase in $d_{s,c}$ to 15 km could occur at approximately constant stress conditions if brittle deformation caused by the earthquake promotes strain localization onto ~1-m-wide shear zones (resulting in a strain rate of 10^{-9} /s) and the resulting dilatancy results in a decrease in λ from 0.95 to 0.8. We emphasize the speculative nature of these analyses and that other processes that control α need to be investigated, such as lithology, metamorphic reactions, sub-critical crack growth, crack healing, and pressure solution. For example, the observation of significant microseismicity below $d_{s,c}$ in Figure 3B would require large stress increases if the quartz flow law is applicable at depths down to 20 km. In contrast, if the effective viscosity at these depths is greater, owing to lithological variations (controlled by plagioclase, for example), α would be higher and brittle deformation would be possible at lower stresses.

CONCLUSION

Natural and laboratory observations suggest that the effective stress law must become “ineffective” at some mid-crustal conditions. Our simple, physically motivated contact-scale model results in an effective stress equation that qualitatively explains the observations. This model may also provide new insights for understanding stress, deformation, and seismicity near the brittle-ductile transition and in the broad transition zone that occurs on the deep segments of some plate-boundary faults. For example, tidal triggering of the deep crustal tremor along the San Andreas fault is difficult to explain without calling on low shear stresses resulting from low effective normal stresses associated with high pore-fluid pressures (i.e., $\alpha \approx 1$) (e.g., Thomas et al., 2012). In contrast, based on the arguments outlined above, we suspect that α decreases significantly in many high-temperature environments where viscous creep is expected to be dominant or at least competitive with brittle processes. The model proposed here provides a context to investigate how the effective pressure law evolves with variations in lithology (through its effects on asperity rheology), tectonic environment, strain rate, and the evolution of pore-fluid pressure.

ACKNOWLEDGMENTS

This work was funded through grants from the National Science Foundation and the Southern California Earthquake Center. We thank A. Thomas and R. Burgmann for helpful discussions, and C. Morrow, P. McCrory, J. Platt (University of Southern California), M. Handy, and D. Wallis for constructive reviews.

REFERENCES CITED

Axen, G.J., Selverstone, J., and Wawrzyniec, T., 2001, High-temperature embrittlement of extensional Alpine mylonite zones in the midcrustal ductile-brittle transition: *Journal of Geophysical Research*, v. 106, p. 4337–4348, doi:10.1029/2000JB900372.

Behr, W.M., and Platt, J.P., 2011, A naturally constrained stress profile through the middle crust in an extensional terrane: *Earth and Planetary Science Letters*, v. 303, p. 181–192, doi:10.1016/j.epsl.2010.11.044.

Boettcher, M., Hirth, G., and Evans, B., 2007, Olivine friction at the base of oceanic seismogenic zones: *Journal of Geophysical Research*, v. 112, B01205, doi:10.1029/2006JB004301.

Brace, W.F., and Kohlstedt, D.L., 1980, Limits on lithospheric stress imposed by laboratory experiments: *Journal of Geophysical Research*, v. 85, p. 6248–6252, doi:10.1029/JB085iB11p06248.

Bürgmann, R., and Dresen, G., 2008, Rheology of the lower crust and upper mantle: Evidence from rock mechanics, geodesy, and field observations: *Annual Review of Earth and Planetary Sciences*, v. 36, p. 531–567, doi:10.1146/annurev.earth.36.031207.124326.

Chernak, L., Hirth, G., Selverstone, J., and Tullis, J., 2009, The effect of aqueous and carbonic fluids on the dislocation creep strength of quartz: *Journal of Geophysical Research*, v. 114, B04201, doi:10.1029/2008JB005884.

Dieterich, J.H., and Kilgore, B.D., 1996, Imaging surface contacts: Power law contact distributions and contact stresses in quartz, calcite, glass and acrylic plastic: *Tectonophysics*, v. 256, p. 219–239, doi:10.1016/0040-1951(95)00165-4.

Dresen, G., Duyster, J., Stöckhert, B., Wirth, R., and Zulauf, G., 1997, Quartz dislocation microstructure between 7000 m and 9100 m depth from the Continental Deep Drilling Program KTB: *Journal of Geophysical Research*, v. 102, p. 18,443–18,452, doi:10.1029/96JB03394.

Evans, B., 1984, The effect of temperature and impurity content on indentation hardness of quartz: *Journal of Geophysical Research*, v. 89, p. 4213–4222, doi:10.1029/JB089iB06p04213.

Handin, J., Hager, R.V., Friedman, M., and Feathers, J.N., 1963, Experimental deformation of sedimentary rocks under confining pressure: Pore pressure tests: *Bulletin of the American Association of Petroleum Geologists*, v. 5, p. 716–755.

Handy, M.R., Hirth, G., and Burgmann, R., 2007, Continental fault structure and rheology from the frictional-to-viscous transition downward, in Handy, M.R., et al., eds., *Tectonic Faults: Agents of Change on a Dynamic Earth*: Cambridge, Massachusetts, MIT Press, p. 139–181.

Hirth, G., and Kohlstedt, D.L., 1995, Experimental constraints on the dynamics of the partially molten upper mantle: Deformation in the diffusion creep regime: *Journal of Geophysical Research*, v. 100, p. 1981–2001, doi:10.1029/94JB02128.

Hirth, G., Teyssier, C., and Dunlap, W.J., 2001, An evaluation of quartzite flow laws based on comparisons between experimentally and naturally deformed rocks: *International Journal of Earth Sciences (Geologische Rundschau)*, v. 90, p. 77–87.

Hubbert, M.K., and Rubey, W.W., 1959, Role of fluid pressure in mechanics of overthrust faulting: *Geological Society of America Bulletin*, v. 70, p. 115–160, doi:10.1130/0016-7606(1959)70[115:ROFPIM]2.0.CO;2.

Humphreys, E.D., and Coblenz, D.D., 2007, North American dynamics and Western U.S. tectonics: *Reviews of Geophysics*, v. 45, p. 1–30.

Montési, L., 2004, Postseismic deformation and the strength of ductile shear zones: *Earth, Planets, and Space*, v. 56, p. 1135–1142, doi:10.1186/BF03353332.

Morrow, C., Radney, B., and Byerlee, J., 1992, Frictional strength and the effective pressure law of montmorillonite and illite clays: *International Geophysics*, v. 51, p. 69–88, doi:10.1016/S0074-6142(08)62815-6.

Powers, P.M., and Jordan, T.H., 2010, Distribution of seismicity across strike-slip faults in California: *Journal of Geophysical Research*, v. 115, B05305, doi:10.1029/2008JB006234.

Renner, J., Viskupic, K., Hirth, G., and Evans, B., 2003, Melt extraction from partially molten peridotite: *Geochemistry Geophysics Geosystems*, v. 4, 8606, doi:10.1029/2002GC000369.

Rolandone, F., Burgmann, R., and Nadeau, R.M., 2004, The evolution of the seismic-aseismic transition during the earthquake cycle: Constraints from the time-dependent depth distribution of aftershocks: *Geophysical Research Letters*, v. 31, L23610, doi:10.1029/2004GL021379.

Scholz, C.H., 1990, *The Mechanics of Earthquakes and Faulting*: Cambridge, UK, Cambridge University Press, 471 p.

Sibson, R.H., 1983, Continental fault structure and the shallow earthquake source: *Journal of the Geological Society*, v. 140, p. 741–767, doi:10.1144/gsjgs.140.5.0741.

Stipp, M., Stunitz, H., Heilbronner, R., and Schmid, S.M., 2002, The eastern Tonale fault zone: A ‘natural laboratory’ for crystal plastic deformation of quartz over a temperature range from 250 to 700 °C: *Journal of Structural Geology*, v. 24, p. 1861–1884, doi:10.1016/S0191-8141(02)00035-4.

Takei, Y., and Holtzman, B.K., 2009, Viscous constitutive relations of solid-liquid composites in terms of grain boundary contiguity: 2. Compositional model for small melt fractions: *Journal of Geophysical Research*, v. 114, B06206, doi:10.1029/2008JB005851.

Thomas, A.M., Burgmann, R., Shelly, D.R., Beeler, N.M., and Rudolph, M.L., 2012, Tidal sensitivity of low frequency earthquakes near Parkfield, California: Implications for fault mechanics within the brittle-ductile transition: *Journal of Geophysical Research*, v. 117, B05301, doi:10.1029/2011JB009036.

Zoback, M.D., and Townend, J., 2001, Implication of hydrostatic pore pressures and high crustal strength for the deformation of intraplate lithosphere: *Tectonophysics*, v. 336, p. 19–30, doi:10.1016/S0040-1951(01)00091-9.

Manuscript received 16 October 2014

Revised manuscript received 10 December 2015

Manuscript accepted 15 December 2014

Printed in USA